Published in final edited form as:
Ann Surg Oncol. 2014 December ; 21(0 4): 528–537. doi:10.1245/s10434-014-3524-x.

Near-infrared Fluorescent Imaging of Both Colorectal Cancer and Ureters Using a Low-Dose Integrin Targeted Probe

Floris P.R. Verbeek, M.Sc.[1,*], **Joost R. van der Vorst, M.D.**[1,*], **Quirijn R.J.G. Tummers, M.D.**[1], **Martin C. Boonstra, B.Sc.**[1], **Karien E. de Rooij, Ph.D.**[2,4], **Clemens W.G.M. Löwik, Ph.D.**[2], **A. Rob P.M. Valentijn, Ph.D.**[3], **Cornelis J.H. van de Velde, M.D., Ph.D.**[1], **Hak Soo Choi, Ph.D.**[5], **John V. Frangioni, M.D., Ph.D.**[5,6], and **Alexander L. Vahrmeijer, M.D., Ph.D**[1]

[1]Leiden University Medical Center, Leiden, the Netherlands, Department of Surgery [2]Leiden University Medical Center, Leiden, the Netherlands, Department of Radiology [3]Leiden University Medical Center, Leiden, the Netherlands, Department of Clinical Pharmacology and Toxicology [4]Percuros B.V., Leiden, the Netherlands [5]Beth Israel Deaconess Medical Center/Harvard Medical School, Boston, MA 02215, Department of Medicine, Division of Hematology/Oncology [6]Beth Israel Deaconess Medical Center/Harvard Medical School, Boston, MA 02215, Department of Radiology

Abstract

Background—Irradical tumor resections and iatrogenic ureteral injury remain a significant problem during lower abdominal surgery. The aim of the current study was to intraoperatively identify both colorectal tumors and ureters in subcutaneous and orthotopic animal models using cRGD-ZW800-1 and NIR fluorescence.

Methods—The zwitterionic fluorophore ZW800-1 was conjugated to the tumor specific peptide cRGD (targeting integrins) and to the a-specific peptide cRAD. One nmol cRGD-ZW800-1, cRAD-ZW800-1, or ZW800-1 alone was injected in mice bearing subcutaneous HT-29 human colorectal tumors. Subsequently, cRGD-ZW800-1 was injected at dosages of 0.25 and 1 nmol in mice bearing orthotopic HT-29 tumors transfected with luciferase2. *In vivo* biodistribution and

Corresponding author: Dr. Alexander L. Vahrmeijer, M.D., Ph.D., Albinusdreef 2, 2300 RC Leiden, Phone: +31715262309, Fax: +31715266750, a.l.vahrmeijer@lumc.nl.
*Both authors contributed equally to this work and share first-authorship.

Disclosures: Floris P.R. Verbeek, M.Sc.: None
Joost R. van der Vorst, M.D.: None
Quirijn R.J.G. Tummers, M.D.: None
Martin C. Boonstra, B.Sc.: None
Karien E. de Rooij, Ph.D.: None
Clemens W.G.M. Löwik, Ph.D.: None
A. Rob P.M. Valentijn, Ph.D.: None
Cornelis J.H. van de Velde, M.D., Ph.D.: None
Hak Soo Choi, Ph.D.: None
John V. Frangioni, M.D., Ph.D.: FLARE™ technology is owned by Beth Israel Deaconess Medical Center, a teaching hospital of Harvard Medical School. Dr. Frangioni has started three for-profit companies, Curadel, Curadel ResVet Imaging, and Curadel Surgical Innovations, which has optioned FLARE™ technology for potential licensing from Beth Israel Deaconess Medical Center.
Alexander L. Vahrmeijer, M.D., Ph.D.: None

ureteral visualization were investigated in rats. Fluorescence was measured intraoperatively at several time points after probe administration using the FLARE imaging system.

Results—Both subcutaneous and orthotopic tumors could be clearly identified using cRGD-ZW800-1. A significantly higher signal-to-background ratio (SBR) was observed in mice injected with cRGD-ZW800-1 (2.42 ± 0.77) compared to mice injected with cRAD-ZW800-1 or ZW800-1 alone (1.21 ± 0.19 and 1.34 ± 0.19, respectively) when measured at 24 h after probe administration. The clearance of cRGD-ZW800-1 permitted visualization of the ureters and also generated minimal background fluorescence in the gastrointestinal tract.

Conclusions—This study appears to be the first to demonstrate both clear tumor demarcation and ureteral visualization after a single intravenous injection of a targeted NIR fluorophore. As a low dose of cRGD-ZW800-1 provided clear tumor identification, clinical translation of these results should be possible.

Keywords

Near-Infrared Fluorescence Imaging; Image-Guided Surgery; colorectal cancer; ureteral damage; integrin; ureteral visualization

Introduction

In cancer surgery, positive resection margins remain one of the biggest problems, resulting in a high number of recurrences and poor prognosis. In contrast to the many imaging modalities that can be used preoperatively for diagnosis, staging, and surgical planning (CT, MRI, SPECT, PET), real-time, intraoperative imaging modalities to assess the extent of disease and to determine adequate resection margins are lacking. In most cases, surgeons still have to rely only on palpation and visual inspection to discriminate between tumor tissue and normal tissue [1]. Since this situation has not been changed for many decades, there remains a need for a diagnostic tool that can discriminate tumor tissue from normal tissue in real time during surgery.

In addition, iatrogenic ureteral injury is a rare, but serious complication of lower abdominal surgery, with a reported incidence rate varying from 0.7% up to 10% [2-4]. Ureteral identification can be challenging, especially in patients with previous surgery or inflammation, and during minimally invasive procedures. Early identification of ureteral damage permits direct repair and is of paramount importance to reduce morbidity and preservation of renal function.

Near-infrared (NIR) fluorescence guided surgery is a novel technique that enables real-time visualization of tumors and vital structures (i.e. ureters) using light in the NIR spectrum [5-7]. The use of NIR light has the advantages of being less absorbed by tissue and being invisible to the human eye. This results in high tissue penetration without altering the look of the surgical field. By conjugating NIR fluorescent dyes to tumor specific ligands, intraoperative NIR fluorescent tumor detection and demarcation can be achieved. During the last decade, many tumor-specific ligands, such as antibodies, nanobodies, and peptides have been used for this purpose, all with their own advantages and disadvantages [8-11]. Furthermore, multiple fluorescent dyes have been tested to optimize fluorescent intensity, biodistribution, and

clearance [12-15]. In addition, Metildi et. al. recently showed the ability to visualize sub-millimeter tumor deposits along the cecal wall in a patient-derived orthotopic nude mouse model using a chimeric CEA antibody and visible fluorescence [16].

The present study evaluates the use of a low dose fluorescent dye ZW800-1 conjugated to the cyclic RGD peptide (cRGD) targeting integrin for colorectal tumor imaging and ureteral visualization [15]. RGD is a small peptide that targets integrin α5β1, α8β1, αvβ1, αvβ3, αvβ5, αvβ6, αvβ8 and αIIbβ3 [17-20]. Integrins are cell-surface transmembrane heterodimeric glycoproteins that are involved in cell adhesion, matrix interaction, and cell signaling pathways [21]; integrin $\alpha_v\beta_3$ plays a key role in the early phase of tumor angiogenesis, tumor cell migration, and is overexpressed in various cancer types, including colorectal and breast cancer [22]. Moreover, an intermediate to high expression of αvβ3 is observed on the (neo)vasculature of colon carcinoma in about 75% of patients with colon cancer [23, 24]. cRGD-ZW800-1 has recently been developed and validated by our group using *in vitro and in vivo* assays with melanoma, breast, liver and lung cancer cell lines [15]. In addition, recent preclinical studies demonstrated successful identification of breast, colon, lung, ovarian, and glioblastoma cancers by targeting $\alpha_v\beta_3$ integrin [25-29]. Furthermore, a number of clinical studies successfully showed integrin $\alpha_v\beta_3$ targeting using ^{18}F-galacto-RGD and PET imaging in breast cancer and malignant gliomas [28, 30-32].

ZW800-1 is a recently developed zwitterionic fluorescent dye which is cleared rapidly by the kidneys, has a high quantum yield, and was engineered for high hydrophilicity [33]. ZW800-1 has a net charge of 0 after conjugation to a targeting ligand with a net charge of -1 prior to conjugation, an absorption peak of approximately 772 nm, and an emission peak of 788 nm in fetal bovine serum. ZW800-1 is freely filtered by the kidney and is exclusively eliminated from the body by the kidneys. As such, non-specific background signal in the intestines is low, making it valuable for colorectal tumor imaging, and simultaneously, ureteral visualization is enabled. To maximize renal clearance of the conjugate, the hydrophilic variant RGDyK was chosen for conjugation to ZW800-1 [34].

The aim of the current study was to evaluate the ability to visualize both colorectal cancer and ureters using NIR fluorescence and a single injection of cRGD-ZW800-1.

Methods

Ethical standards and animal care

All animal experiments were approved for animal health, ethics, and research by the Animal Welfare Committee of Leiden University Medical Center, the Netherlands. All animals received humane care and maintenance in compliance with the “Code of Practice Use of Laboratory Animals in Cancer Research” (Inspectie W&V, July 1999). All animals were housed in the animal facility of the Leiden University Medical Center. Pellet food and fresh tap water were provided *ad libitum*. The weight of the animals was followed throughout the experiment to monitor their general health state. Throughout tumor inoculation, imaging, and surgical procedures, the animals were anesthetized with 5% isoflurane for induction and 2% isoflurane for maintenance in oxygen with a flow of 0.8 L/min and placed on an animal bed with an integrated nose mask.

Tumor models

Subcutaneous colon tumors were induced in 6 week-old CD1-Foxn1^{nu} female mice (Charles River Laboratories, Wilmington, MA, USA) weighing 25 - 35 g by subcutaneous injection at 4 sites with 5×10^5 HT29-luc2 cells in 40 μL RPMI1640 medium per site. Tumor growth was monitored longitudinally using a digital caliper and with bioluminescence imaging (BLI) after an intraperitoneal injection of 150 mg/kg of D-luciferin solution (SynChem, Inc., Elk Grove Village, IL) in PBS in a total volume of 50 μL 10 minutes prior to imaging using the IVIS Spectrum imaging system (Caliper LifeSciences, Hopkinton, MA, USA). In order to induce orthotopic tumors, subcutaneously growing HT29-luc2 colon tumors were harvested and subsequently transplanted onto the cecum of a healthy mouse, according to the model described by Tseng et al. [35] (fig. 4a). Briefly, the cecal wall was slightly incised to facilitate tumor cell infiltration and small tumor fragments (approximately 2 mm) were transplanted on the cecal wall using a 6-0 suture. Tumor growth was monitored using BLI.

In Vivo biodistribution and ureteral visualization

The ability to visualize gastrointestinal tumors in close proximity to other organs was investigated in nude mice bearing orthotopic HT29 tumors. As cRGD-ZW800-1 is cleared renally, a single intravenous injection could potentially also permit ureteral visualization. However, it showed to be challenging to visualize the ureter in nude mice **weighing** only 25-35 g. Therefore, to validate *in vivo* biodistribution and ureteral visualization, cRGD-ZW800-1 was also administered to male WAG/Rij rats (Harlan, Horst, The Netherlands) **weighing** approximately 300–350 g.

NIR fluorescence imaging

When tumors were measured 5 mm in diameter, the fluorescent probe was injected. 1 nmol cRGD-ZW800-1 (N = 3), 1 nmol cRAD-ZW800-1 (N = 3), or 1 nmol ZW800-1 (N = 3) was injected intravenously in mice bearing subcutaneous tumors. NIR fluorescent signal was measured at 0.3, 0.5, 1, 2, 4, 8, 24, and 48 h after injection using the FLARE imaging system and signal-to-background ratios were calculated. Subsequently, cRGD-ZW800-1 was injected at dosages of 1 and 0.25 nmol in mice with orthotopically transplanted cecal tumors (N = 6). To observe *in vivo* biodistribution and ureteral visualization, 30 nmol cRGD-ZW800-1 was injected intravenously in 3 Wag/Rij rats. After injection, NIR fluorescent signal of the liver, small bowel, colon, kidney, and bladder was measured over time. NIR fluorescence measurements were performed using the FLARE imaging system as described before [36].

Histological analysis

Subcutaneous tumors were surgically removed and processed. Snap frozen tissue was sectioned at 6 μm and was scanned on the Odyssey Infrared Imaging System (LI-COR Biosciences, Lincoln, NE) using the 800 nm channel. Subsequently sections were stained using a hematoxylin and eosin to make an overlay.

Statistical Analysis

For statistical analysis, SPSS statistical software package (Version 17.0, Chicago, IL) was used. To generate graphs, GraphPad Prism Software (Version 5.01, La Jolla, CA) was used. Signal-to-background ratios (SBR) were calculated by dividing the fluorescent signal of the tumor by fluorescent signal of surrounding tissue. SBR was reported in mean and standard deviation. To compare SBRs between dose groups and time points, and to assess the relation between dose and time, a mixed model analysis was used. When a significant difference was detected, a one-way ANOVA was used to post-test for differences between separate dose groups and/or time points. The one-way ANOVA was corrected using the Bonferroni correction. $P < 0.05$ was considered significant.

Results

NIR fluorescent probe

cRGD and cRAD were conjugated to ZW800-1 as described in the supplementary data (Fig. 1). Purity (> 98%) was confirmed by analytical reversed-phase HPLC (770 nm absorbance) and MALDI-TOF.

Intraoperative NIR Fluorescence Imaging Mice with Subcutaneous tumors

Three weeks after inoculation, mice were injected intravenously with cRGD-ZW800-1, cRAD-ZW800-1, or ZW800-1 alone. All subcutaneous tumors of mice could be clearly identified after injection of cRGD-ZW800-1 using NIR fluorescence (SBR at 24 h after injection was 2.42 ± 0.77; Fig. 2). No adequate tumor-to-background ratios were observed in the control mice injected with cRAD-ZW800-1 (SBR was 1.21 ± 0.19 at 24 h after injection) or ZW800-1 alone (SBR was 1.34 ± 0.19 at 24 h after injection). Using a mixed-model analysis, differences in SBRs between 3 study groups and between time points were significant ($P = 0.006$ and $P < 0.0001$, respectively; Fig. 2). Post-testing using a one-way ANOVA showed significant differences between the cRGD-ZW800-1 and the cRAD-ZW800-1 ($P < 0.0001$) study groups and between the cRGD-ZW800-1 and ZW800-1 alone ($P < 0.0001$) study groups. No significant difference was found between cRAD-ZW800-1 and ZW800-1 alone ($P = 1.0$). The highest SBRs were measured at 8 (2.33 ± 0.68) and 24 h (2.42 ± 0.77) after administration of cRGD-ZW800-1.

Histological analysis

Using the Odyssey Infrared Imaging System, clear differences were observed between 3 study groups. An increased fluorescent signal was observed in tumors harvested from mice in which cRGD-ZW800-1 was injected and a weak fluorescent signal was measured in tumors harvested from mice in the control groups (cRAD-ZW800-1 and ZW800-1 alone) (Fig. 3).

Intraoperative NIR Fluorescence Imaging in Mice with Orthotopic Tumors

In 6 mice with orthotopically transplanted colon tumors, tumor growth was assessed using BLI (Fig. 4b). After 30 days, BLI measurements showed approximately 5.0×10^6 counts and cRGD-ZW800-1 was administered intravenously. cRGD-ZW800-1 was administered at

dosages of 1 (N = 3) and 0.25 nmol (N = 3) (Fig. 4c). In all mice, tumors could be adequately differentiated from surrounding healthy bowel tissue (Fig. 4c and d). Average SBR in these mice was 2.62 ± 0.17 and 1.75 ± 0.36 for the 1 and 0.25 nmol dose groups respectively.

In vivo Biodistribution and Ureteral Visualization in Rats

To assess the potential use of cRGD-ZW800-1 for both intraoperative detection of gastrointestinal tumors and ureteral identification, the NIRF intensity of abdominal organs was quantified over time in 3 male Wag/Rij rats. After administration of cRGD-ZW800-1 intravenously, medial laparotomy was performed and signal in liver, small bowel, colon, kidney, and bladder was measured. Time points were 0, 0.1, 0.5, 1, 2, 3, 4, 8, and 24 h after intravenous administration (fig. 5). Average fluorescence intensities (normalized arbitrary units, AU) at t = 2 hour, were: 594 (± 163), 599 (± 65), 443 (± 169), 6172 (± 3250) and 21714 (± 2102) for the liver, small bowel, colon, kidney, and bladder respectively. Figure 5a shows an example in which the ureters could clearly be visualized, 30 minutes after injection of cRGD-ZW800-1.

Discussion

The present study reports the use of a ligand (cRGD) conjugated to ZW800-1 that targets integrins in low dosage range for NIR fluorescence imaging during surgery. cRGD-ZW800-1 was successfully used in both subcutaneous and orthotopic mouse models to identify malignant cells. Because contrast agents can accumulate in tumors via enhanced permeability and retention (EPR) [37-41], 2 negative control groups (cRAD-ZW800-1 and ZW800-1 alone) were included to confirm specificity of the fluorescent signal in tumors.

With regards to an oncologic resection, in which all tumor cells need to be resected, a specific NIR fluorescent signal is vital. We aimed to develop a fluorescent agent with a low non-specific tumor accumulation component and high specific targeting. Choi et al. recently published the use of the targeted zwitterionic near-infrared fluorophore cRGD-ZW800-1 and compared it with commercially available fluorophores [15]. It was shown that cRGD-ZW800-1 outperformed the commercially available dyes *in vitro* for immunocytometry, histopathology and immunoblotting and *in vivo* for image-guided surgery. However, as this was not the design of the study, no negative controls were used in *in vivo* image-guided surgery models. Therefore, the current study aimed to test the specificity of cRGD-ZW800-1. Mice injected with cRAD-ZW800-1 or ZW800-1 alone showed no tumor signal both during *in vivo* imaging using the FLARE imaging system and *ex vivo* imaging using the Odyssey imaging system. Since cRGD-ZW800-1 and cRAD-ZW800-1 are comparable with regards to size, charge, and solubility, it can be stated that it's highly probable that the cRGD-ZW800-1 signal is specific.

Imaging in the peritoneal cavity can be challenging, mostly due to high levels of background fluorescence when tracers are cleared by the liver. In this study, high tumor-to-background ratios were observed in the orthotopic tumor model due to the low hepatic clearance and the resulting low fluorescent signal in the gastrointestinal tract.

Since cRGD-ZW800-1 is cleared renally, it permits ureteral visualisation in addition to tumor imaging. Noninvasive detection of the ureters using NIR fluorescence has several advantages over conventional ureteral stent placing as it can be used within minutes after dye administration during both open and laparoscopic surgery. Besides, placement of ureteral stents is an invasive procedure that harbors an increased risk of complications such as ureteral perforation, urinary tract infection, and acute renal failure. Clinical feasibility to identify the ureters using NIR imaging has recently been demonstrated [42]. Using cRGD-ZW800-1 for both tumor and ureter imaging during lower abdominal procedures, surgical outcome could be greatly improved, while reducing morbidity. Furthermore, this technique will be of even greater value in laparoscopic surgery as no tactile information can be used. To date, several laparoscopic imaging systems are commercially available, however, further technical developments are in progress to facilitate optimal real-time NIR fluorescence guidance in relation to surgical anatomy [43, 44].

Since cRGD has been extensively used for clinical imaging studies [45, 46], toxicity and safety data are more available when compared to newly synthesized ligands. In these clinical studies, galacto-cRGD was conjugated to fluorodeoxyglucose (^{18}F). However, as cRGD (yK) is more hydrophilic compared to galacto-RGD, the cRGDyK variant was used in this study and will be used for clinical translation.

Another advantage of cRGD-ZW800-1 is that it permits clear tumor and ureteral visualization at low dosages compared to current FDA/EMA approved NIR fluorophores (ICG and Methylene blue). When the dosages used in mice and rats are converted by body surface area, 0.25, 1, and 30 nmol is equivalent to a total human dose of 0.096, 0.39, and 1.33 mg respectively. These dosages are much lower compared to the commonly used amounts of ICG (10-25 mg) and methylene blue (15-60 mg). In addition, a dose of 0.25 nmol in mice corresponds to a human equivalent dose of < 100 μg, which is below the FDA threshold for micro-dosing and portends more rapid clinical translation [47, 48].

In conclusion, the present study reports the use of a recently developed fluorescent probe with minimal background uptake in the gastrointestinal tract. cRGD-ZW800-1 showed clear uptake in both a subcutaneous and an orthotopic colon cancer mouse model. Moreover, as cRGD-ZW800-1 is cleared renally, ureteral visualization is feasible after a single injection. As a low probe dose was used, clinical translation of these results is possible.

Acknowledgments

We thank Hendrica A.J.M. Prevoo for her contribution the histological analysis and David J. Burrington, Jr. for editing. This work was supported in part by the National Institutes of Health grant R01-CA-115296, R01-EB-011523, and R01-EB-010022, Dutch Cancer Society grant UL2010-4732 and the “drie lichten” foundation; the content of this paper is solely the responsibility of the authors and does not necessarily represent the official views of the National Institutes of Health. This study was performed within the framework of the Center of Translational Molecular Medicine (project MUSIS, grant 03O-202-04 and DeCoDe project, grant 03O-101). Joost van der Vorst is an MD-medical research trainee funded by The Netherlands Organisation for Health Research and Development (grant 92003593).

References

1. Vahrmeijer AL, Frangioni JV. Seeing the invisible during surgery. Br J Surg. 2011; 98(6):749–750. [PubMed: 21484776]
2. Selzman AA, Spirnak JP. Iatrogenic ureteral injuries: a 20-year experience in treating 165 injuries. J Urol. 1996; 155(3):878–881. [PubMed: 8583597]
3. Delacroix SE Jr, Winters JC. Urinary tract injuries: recognition and management. Clin Colon Rectal Surg. 2010; 23(3):221. [PubMed: 21886472]
4. Preston JM. Iatrogenic ureteric injury: common medicolegal pitfalls. BJU Int. 2000; 86(3):313–317. [PubMed: 10930939]
5. Frangioni JV. In vivo near-infrared fluorescence imaging. Curr Opin Chem Biol. 2003; 7(5):626–634. [PubMed: 14580568]
6. Vahrmeijer AL, Hutteman M, van der Vorst JR, van de Velde CJ, Frangioni JV. Image-guided cancer surgery using near-infrared fluorescence. Nat Rev Clin Oncol. 2013
7. Pleijhuis RG, Graafland M, de VJ, Bart J, de jong JS, van Dam GM. Obtaining adequate surgical margins in breast-conserving therapy for patients with early-stage breast cancer: current modalities and future directions. Ann Surg Oncol. 2009; 16(10):2717–2730. [PubMed: 19609829]
8. Oliveira S, van Dongen GA, Stigter-van WM, et al. Rapid visualization of human tumor xenografts through optical imaging with a near-infrared fluorescent anti-epidermal growth factor receptor nanobody. Mol Imaging. 2012; 11(1):33–46. [PubMed: 22418026]
9. Themelis G, Harlaar NJ, kelder W, et al. Enhancing surgical vision by using real-time imaging of alphavbeta3-integrin targeted near-infrared fluorescent agent. Ann Surg Oncol. 2011; 18(12):3506–3513. [PubMed: 21509632]
10. Heath CH, Deep NL, Sweeny L, Zinn KR, Rosenthal EL. Use of panitumumab-IRDye800 to image microscopic head and neck cancer in an orthotopic surgical model. Ann Surg Oncol. 2012; 19(12):3879–3887. [PubMed: 22669455]
11. Metildi CA, Tang CM, Kaushal S, et al. In Vivo Fluorescence Imaging of Gastrointestinal Stromal Tumors Using Fluorophore-Conjugated Anti-KIT Antibody. Ann Surg Oncol. 2013
12. van der Vorst JR, Hutteman M, Mieog JS, et al. Near-Infrared Fluorescence Imaging of Liver Metastases in Rats using Indocyanine Green. J Surg Res. 2011; 174(266):271.
13. Keereweer S, Mol IM, Vahrmeijer AL, et al. Dual wavelength tumor targeting for detection of hypopharyngeal cancer using near-infrared optical imaging in an animal model. Int J Cancer. 2012; 131(7):1633–1640. [PubMed: 22234729]
14. Wu Y, Cai W, Chen X. Near-infrared fluorescence imaging of tumor integrin alpha v beta 3 expression with Cy7-labeled RGD multimers. Mol Imaging Biol. 2006; 8(4):226–236. [PubMed: 16791749]
15. Choi HS, Gibbs SL, Lee JH, et al. Targeted zwitterionic near-infrared fluorophores for improved optical imaging. Nat Biotechnol. 2013; 31(2):148–153. [PubMed: 23292608]
16. Metildi CA, Kaushal S, Luiken GA, Talamini MA, Hoffman RM, Bouvet M. Fluorescently labeled chimeric anti-CEA antibody improves detection and resection of human colon cancer in a patient-derived orthotopic xenograft (PDOX) nude mouse model. J Surg Oncol. 2013
17. Bunschoten A, Buckle T, Visser N, et al. Multimodal interventional molecular imaging of tumor margins and distant metastases using the integrin a_vB_3 expression. ChemBioChem. 2012 May 7; 13(7):1039–45. [PubMed: 22505018]
18. Tucker GC. Integrins: molecular targets in cancer therapy. Curr Oncol Rep. 2006; 8(2):96–103. [PubMed: 16507218]
19. Barczyk M, Carracedo S, Gullberg D. Integrins. Cell Tissue Res. 2010; 339(1):269–280. [PubMed: 19693543]
20. Ruoslahti E. RGD and other recognition sequences for integrins. Annu Rev Cell Dev Biol. 1996; 12:697–715. [PubMed: 8970741]
21. Hood JD, Cheresh DA. Role of integrins in cell invasion and migration. Nat Rev Cancer. 2002; 2(2):91–100. [PubMed: 12635172]

22. Vonlaufen A, Wiedle G, Borisch B, Birrer S, Luder P, Imhof BA. Integrin alpha(v)beta(3) expression in colon carcinoma correlates with survival. Mod Pathol. 2001; 14(11):1126–1132. [PubMed: 11706074]
23. Vonlaufen A, Wiedle G, Borisch B, Birrer S, Luder P, Imhof BA. Integrin alpha(v)beta(3) expression in colon carcinoma correlates with survival. Mod Pathol. 2001; 14(11):1126–1132. [PubMed: 11706074]
24. Max R, Gerritsen RR, Nooijen PT, et al. Immunohistochemical analysis of integrin alpha vbeta3 expression on tumor-associated vessels of human carcinomas. Int J Cancer. 1997; 71(3):320–324. [PubMed: 9139861]
25. Axelsson R, Bach-Gansmo T, Castell-Conesa J, McParland BJ. An open-label, multicenter, phase 2a study to assess the feasibility of imaging metastases in late-stage cancer patients with the alpha(v)beta(3)-selective angiogenesis imaging agent (99m)Tc-NC100692. Acta Radiol. 2010; 51(1):40–46. [PubMed: 20001475]
26. Huang R, Vider J, Kovar JL, et al. Integrin alphavbeta3-Targeted IRDye 800CW Near-Infrared Imaging of Glioblastoma. Clin Cancer Res. 2012
27. Edwards WB, Akers WJ, Ye Y, et al. Multimodal imaging of integrin receptor-positive tumors by bioluminescence, fluorescence, gamma scintigraphy, and single-photon emission computed tomography using a cyclic RGD peptide labeled with a near-infrared fluorescent dye and a radionuclide. Mol Imaging. 2009; 8(2):101–110. [PubMed: 19397855]
28. Beer AJ, Kessler H, Wester HJ, Schwaiger M. PET Imaging of Integrin alphaVbeta3 Expression. Theranostics. 2011; 1:48–57. [PubMed: 21547152]
29. Harlaar NJ, kelder W, Sarantopoulos A, et al. Real-time near infrared fluorescence (NIRF) intra-operative imaging in ovarian cancer using an alpha(v)beta(3-)integrin targeted agent. Gynecol Oncol. 2013; 128(3):590–595. [PubMed: 23262209]
30. Beer AJ, Haubner R, Sarbia M, et al. Positron emission tomography using [18F]Galacto-RGD identifies the level of integrin alpha(v)beta3 expression in man. Clin Cancer Res. 2006; 12(13): 3942–3949. [PubMed: 16818691]
31. Beer AJ, Niemeyer M, Carlsen J, et al. Patterns of alphavbeta3 expression in primary and metastatic human breast cancer as shown by 18F-Galacto-RGD PET. J Nucl Med. 2008; 49(2): 255–259. [PubMed: 18199623]
32. Schnell O, Krebs B, Carlsen J, et al. Imaging of integrin alpha(v)beta(3) expression in patients with malignant glioma by [18F] Galacto-RGD positron emission tomography. Neuro Oncol. 2009; 11(6):861–870. [PubMed: 19401596]
33. Choi HS, Nasr K, Alyabyev S, et al. Synthesis and in vivo fate of zwitterionic near-infrared fluorophores. Angew Chem Int Ed Engl. 2011; 50(28):6258–6263. [PubMed: 21656624]
34. Pohle K, Notni J, Bussemer J, Kessler H, Schwaiger M, Beer AJ. 68Ga-NODAGA-RGD is a suitable substitute for (18)F-Galacto-RGD and can be produced with high specific activity in a cGMP/GRP compliant automated process. Nucl Med Biol. 2012; 39(6):777–784. [PubMed: 22444238]
35. Tseng W, Leong X, Engleman E. Orthotopic mouse model of colorectal cancer. J Vis Exp. 2007; (10):484. [PubMed: 18989400]
36. Troyan SL, Kianzad V, Gibbs-Strauss SL, et al. The FLARE intraoperative near-infrared fluorescence imaging system: a first-in-human clinical trial in breast cancer sentinel lymph node mapping. Ann Surg Oncol. 2009; 16(10):2943–2952. [PubMed: 19582506]
37. Intes X, Ripoll J, Chen Y, Nioka S, Yodh AG, Chance B. In vivo continuous-wave optical breast imaging enhanced with Indocyanine Green. Med Phys. 2003; 30(6):1039–1047. [PubMed: 12852527]
38. Keereweer S, Mol IM, Kerrebijn JD, et al. Targeting integrins and enhanced permeability and retention (EPR) effect for optical imaging of oral cancer. J Surg Oncol. 2012; 105(7):714–718. [PubMed: 21952950]
39. Arias JL. Drug targeting strategies in cancer treatment: an overview. Mini Rev Med Chem. 2011; 11(1):1–17. [PubMed: 21235512]

40. Maeda H, Wu J, Sawa T, Matsumura Y, Hori K. Tumor vascular permeability and the EPR effect in macromolecular therapeutics: a review. J Control Release. 2000; 65(1-2):271–284. [PubMed: 10699287]
41. Fang J, Nakamura H, Maeda H. The EPR effect: Unique features of tumor blood vessels for drug delivery, factors involved, and limitations and augmentation of the effect. Adv Drug Deliv Rev. 2011; 63(3):136–151. [PubMed: 20441782]
42. Verbeek FP, van der Vorst JR, Schaafsma BE, et al. Intraoperative near infrared fluorescence guided identification of the ureters using low dose methylene blue: a first in human experience. J Urol. 2013; 190(2):574–579. [PubMed: 23466242]
43. Sherwinter DA. Identification of anomolous biliary anatomy using near-infrared cholangiography. J Gastrointest Surg. 2012; 16(9):1814–1815. [PubMed: 22752550]
44. Verbeek FP, Schaafsma BE, Tummers QR, et al. Optimization of near-infrared fluorescence cholangiography for open and laparoscopic surgery. Surg Endosc. 2013
45. Beer AJ, Haubner R, Goebel M, et al. Biodistribution and pharmacokinetics of the alphavbeta3-selective tracer 18F-galacto-RGD in cancer patients. J Nucl Med. 2005; 46(8):1333–1341. [PubMed: 16085591]
46. Haubner R, Wester HJ, Weber WA, et al. Noninvasive imaging of alpha(v)beta3 integrin expression using 18F-labeled RGD-containing glycopeptide and positron emission tomography. Cancer Res. 2001; 61(5):1781–1785. [PubMed: 11280722]
47. U.S. Department of Health and Human Services, Center for Drug Evaluation and Research. Guidance for industry, investigators, and reviewers exploratory IND studies. Rockville, Md: U.S. Department of Health and Human Services; 2006.
48. Scheuer W, van Dam GM, Dobosz M, Schwaiger M, Ntziachristos V. Drug-based optical agents: infiltrating clinics at lower risk. Sci Transl Med. 2012; 4(134):134ps11.

Synopsis

The aim of the current study was to evaluate the ability to visualize both colorectal cancer and ureters using a single injection of a novel NIR fluorophore.

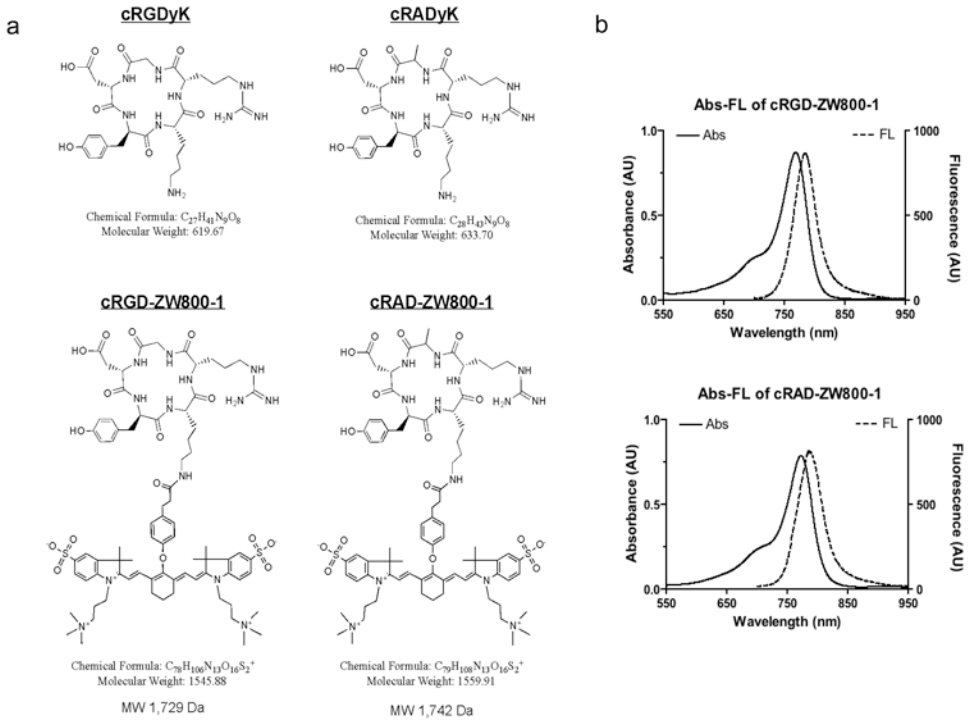

Figure 1. Structure formulas and optical properties

a: Chemical structures and formulae of cRGDyK and cRADyk before and after conjugation to ZW800-1. b: Optical property measurements of cRGD-ZW800-1 and cRAD-ZW800-1.

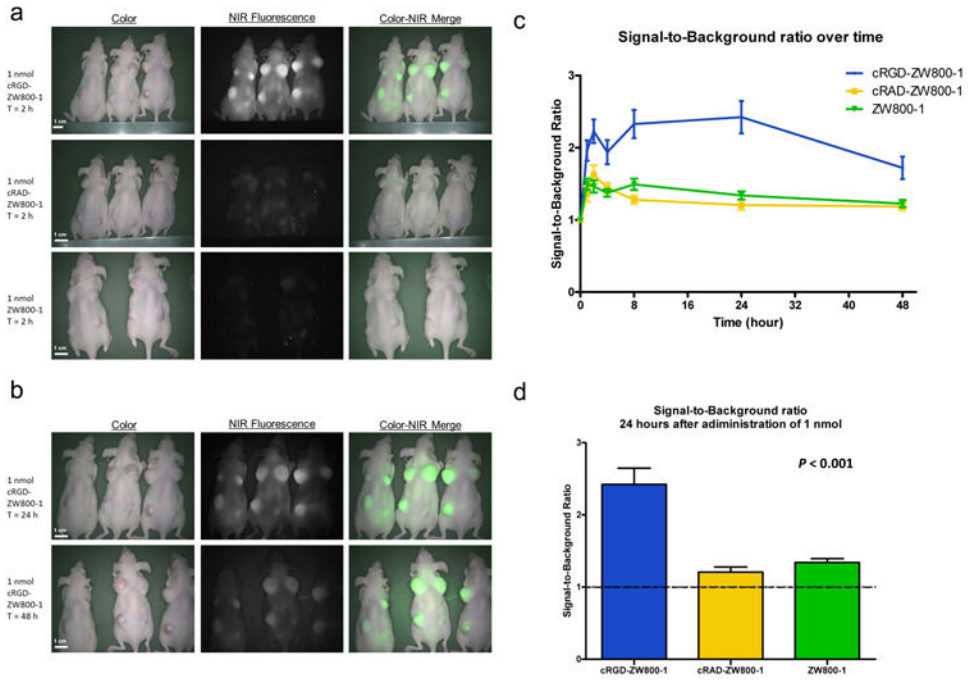

Figure 2. ***In vivo*** **NIR fluorescence imaging of mice bearing subcutaneous tumors**

a: NIR fluorescence imaging of mice bearing subcutaneous HT-29-Luc2 tumors 2 h after administration of 1 nmol cRGD-ZW800-1 (upper row), 1 nmol RAD-ZW800-1 (middle row), and 1 nmol ZW800-1 (lower row). b: NIR fluorescence imaging of the same cRGD-ZW800-1 mice 24 and 48 h after dye administration. Scale bars represent 1 cm. b: Tumor-to-background ratios over time. Plotted are the tumor-to-background ratios (mean, SEM) of cRGD-ZW800-1 (blue line), cRAD-ZW800-1 (yellow), and ZW800-1 alone (green). d: Signal-to-background ratio (mean, SEM) 24 h after administration of 1 nmol of fluorophore.

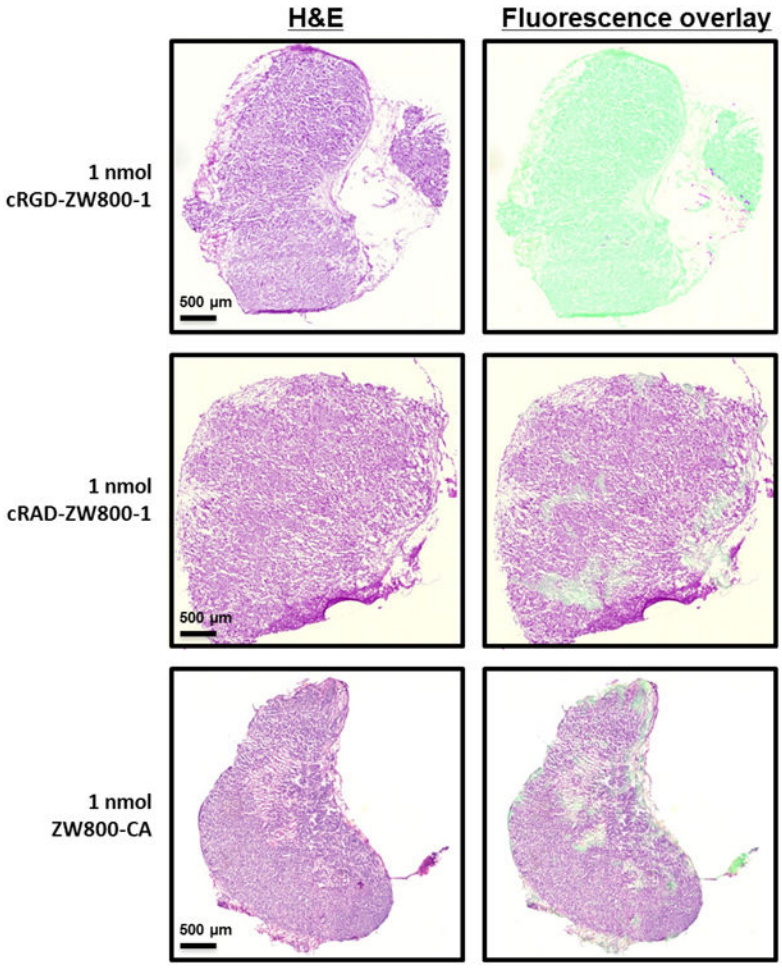

Figure 3. Fluorescence microscopy

Shown are hematoxylin and eosin (H&E) staining (left column) with a pseudo-colored green NIR fluorescence overlay (Odyssey, right column) of a 5 µm tissue section of a subcutaneously growing colon tumor using a 5 × objective. A high fluorescent signal was observed after cRGD-ZW800-1 administration using the Odyssey compared to cRAD-ZW800-1 and ZW800-1. Scale bars represent 500 µm.

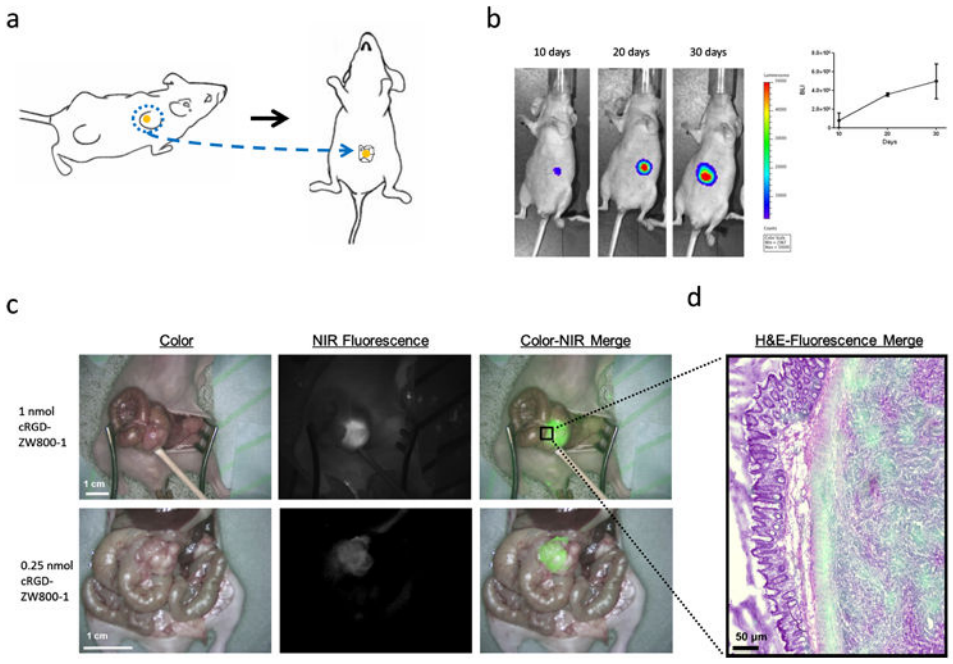

Figure 4. Intraoperative imaging of orthotopic colon tumors

a: Schematic overview of the induction of an orthotopic tumor model. Subcutaneously growing HT29-luc2 colon tumors were resected and transplanted onto the cecum of a healthy mouse. b: tumor growth monitoring using noninvasive bioluminescence imaging. c: Shown are 2 examples of cRGD-ZW800-1 administered intravenously, which allowed clear tumor identification using NIR fluorescence in orthotopic colon tumor bearing mice. cRGD-ZW800-1 was injected at dosages of 1 nmol and 0.25 nmol. Scale bars represent 1 cm. d: H&E and fluorescence overlay of the border between tumor and normal colon tissue.

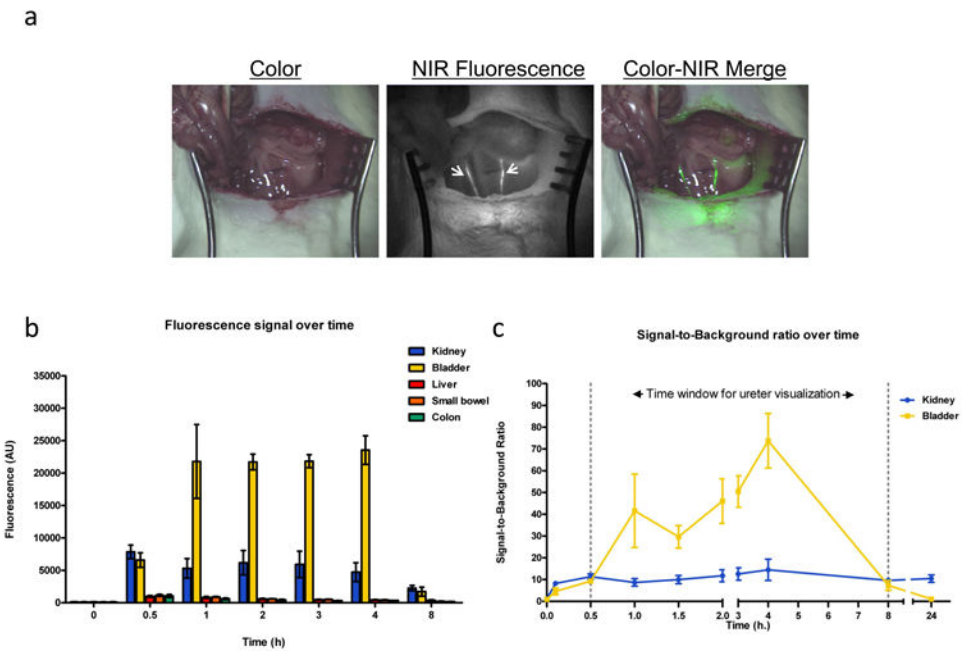

Figure 5. ***In vivo*** **biodistribution and ureteral visualization in rats**

a: Both ureters (arrowheads) could clearly be observed after injection of cRGD-ZW800-1 using NIR fluorescence imaging. b: Fluorescence intensity of abdominal organs was measured using the Mini-FLARE camera system in 3 rats at several time points. c: Signal-to-background ratio of both kidney and ureter is shown over time. Based on these curves the ideal window for ureter visualization appears to lie between 10 min and 8 h. Bars represent mean ± SEM.